

Supplementary Material

for

Live imaging of excitable axonal microdomains in ankyrin-G-GFP mice

Christian Thome^{1,2,3}, Jan Maximilian Janssen^{1,2,4}, Seda Karabulut⁴, Claudio Acuna⁵, Elisa D'Este⁶, Stella J. Soyka⁷, Konrad Baum^{1,2}, Michael Bock⁴, Nadja Lehmann⁴, Johannes Roos^{1,2,4}, Nikolas A. Stevens³, Masashi Hasegawa⁸, Dan A. Ganea⁹, Chloé M. Benoit^{8,9}, Jan Gründemann^{8,9}, Lia Min¹⁰, Kalynn M. Bird¹⁰, Christian Schultz⁴, Vann Bennett¹¹, Paul M. Jenkins^{10*}, Maren Engelhardt^{1,2,4*§}

¹Institute of Anatomy and Cell Biology, Johannes Kepler University, 4020 Linz, Austria

²Clinical Research Institute of Neuroscience, Johannes Kepler University, 4020 Linz, Austria

³Institute of Physiology and Pathophysiology, Heidelberg University, 69120 Heidelberg, Germany

⁴Institute of Neuroanatomy, Mannheim Center for Translational Neuroscience (MCTN), Medical Faculty Mannheim, Heidelberg University, 68167 Mannheim, Germany

⁵Chica and Heinz Schaller Research Group, Institute of Anatomy and Cell Biology, Heidelberg University, 69120 Heidelberg, Germany

⁶Optical Microscopy Facility, Max Planck Institute for Medical Research, 69120 Heidelberg, Germany

⁷Institute of Anatomy and Cell Biology, Dept. of Functional Neuroanatomy, Heidelberg University, 69120 Heidelberg, Germany

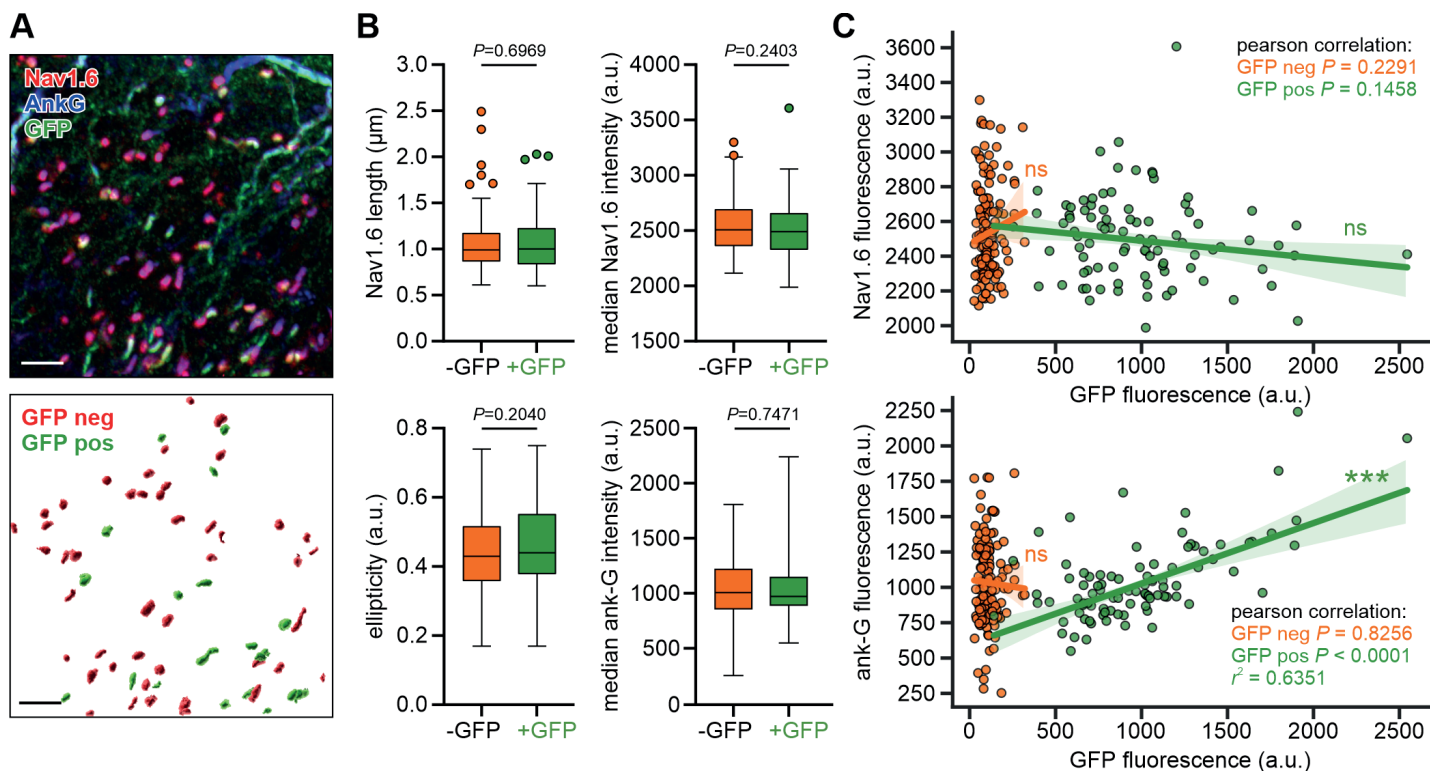
⁸German Center for Neurodegenerative Disease (DZNE), Neural Circuit Computations, 53127 Bonn, Germany

⁹University of Basel, Department of Biomedicine, 4031 Basel, Switzerland

¹⁰Departments of Pharmacology and Psychiatry, University of Michigan Medical School, Ann Arbor, MI 48109, USA

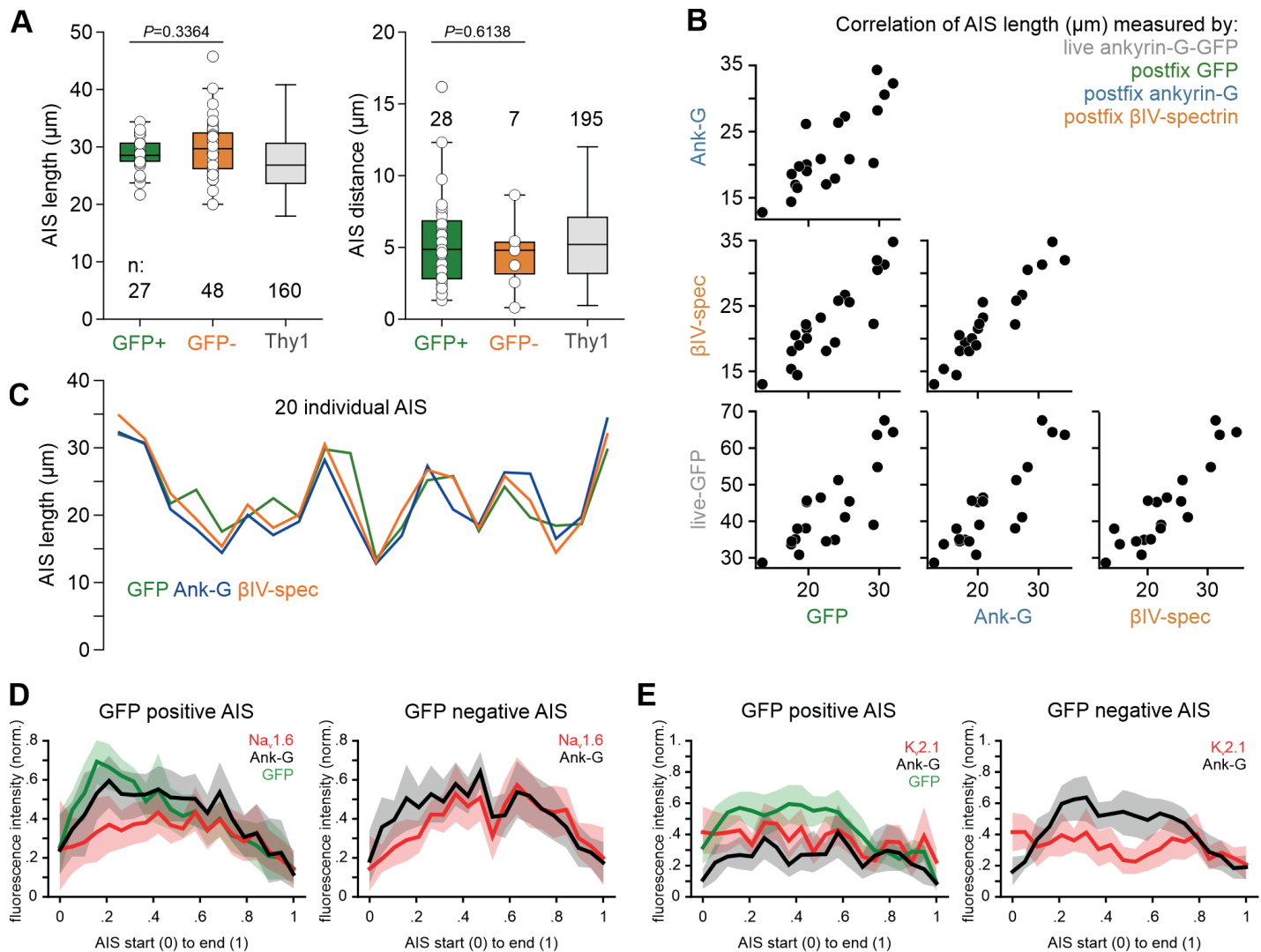
¹¹Department of Biochemistry, Duke University Medical Center, Durham, NC 27710, USA

* These authors contributed equally. § Corresponding author: maren.engelhardt@jku.at



Supplementary Figure S1: Ank-G-GFP activation and expression in nodes of Ranvier do not alter node morphology

A Top panel shows a cryosection of neocortical white matter from an ankyrin-G-GFP x CaMKIIa-Cre mouse, with GFP⁺ and GFP⁻ nodes of Ranvier (noR; see Fig. 3A for details). The bottom panel shows an automated 3D reconstruction of noR using Imaris. Nodes were identified via the ankyrin-G channel, classified by the GFP channel, and properties were analyzed in Na_v1.6 and ankyrin-G channels. All steps were automated within the Imaris software. Scale bar = 5 µm. **B** Nodes that are GFP⁺ and GFP⁻ show no differences regarding their length, ellipticity, and median fluorescence intensity of ankyrin-G or Na_v1.6 signals ($n = 141$ GFP⁻ nodes, 91 GFP⁺ nodes, 1 animal, Mann-Whitney U test). **C** *Top panel*: The fluorescence intensity of the sodium channel Na_v1.6 did not correlate with ankyrin-G-GFP fluorescence intensity, indicating unchanged levels of sodium channels. *Bottom panel*: The intensity of GFP fluorescence correlates positively with the levels of all ankyrin-G in GFP⁺ but not GFP⁻ nodes (n as in B; Pearson correlation details in the graph). This demonstrates that ankyrin-G-GFP does not change the Na_v1.6 channel fluorescence intensity and provides a reliable predictor of ankyrin-G levels, though we do not exclude the possibility that native unlabeled ankyrin-G remains in the nodes to some degree.



Supplementary Figure S2: AIS length, position, and molecular composition remains intact after ankyrin-G-GFP expression

A Measurements of length and position of AIS in CA1 pyramidal neurons that are either GFP positive (green) or negative (orange). The inclusion of GFP into the ankyrin-G gene does not significantly change AIS length (*left* panel) or distance to the soma (*right* panel). Sample preparation was conducted as outlined in Fig. 7 and AIS measurements were based on the $\beta\text{IV-spectrin}$ signal ($n = 3$ animals). An independent Thy1-GFP control line (grey, $n = 3$ animals) was used as an additional control. The number of individual AIS (white circles) and P values are given within the graph (t -test for AIS length; Mann – Whitney U-test for AIS distance). **B** Correlation of AIS length measured live via the ankyrin-G-GFP signal in a patch clamp chamber (grey) and post-fixation using antibodies against GFP, ankyrin-G, and $\beta\text{IV-spectrin}$ in CA1 pyramidal neurons (sample preparation as in Fig. 7, $n = 20$ AIS, 1 animal). **C** Alternative visualization of data from panel B (post-fixation). Measurements for AIS signals using antibodies against GFP, ankyrin-G, and $\beta\text{IV-spectrin}$ show comparable lengths. **D** Immunosignals from Na_v1.6 channels retain their fluorescence intensity across the AIS after the expression of ankyrin-G-GFP. AIS length was normalized from start to end of the ankyrin-G signal and fluorescence intensity from lowest to highest. Tissue preparation as described in Fig. 4A ($n = 10$ GFP⁺ and 10 GFP⁻ AIS). **E** Line plots of K_v2.1 and GFP fluorescence intensities along the AIS signal indicate no change in K_v2.1 expression. Normalization as in panel D. Tissue preparation as described in Fig. 4B ($n = 10$ GFP⁺ and 10 GFP⁻ AIS).

Supplementary Table 1 Summary of statistics for passive and active properties (related to Fig. 7)

stats	wildtype				AnkG-GFP				AnkG-GFP+Cre				ANOVA	
	N	mean	median	SD	N	mean	median	SD	N	mean	median	SD	p(A) / p(KW)	ttest / M-Whit
RMP	28	-63.29	-63.56	3.78	22	-62.57	-63.43	4.62	42	-64.14	-63.32	4.17	0.3441	0.1733
Rinput	28	268.60	251.50	95.51	23	226.10	203.70	89.55	42	253.00	234.40	95.75	<u>0.0952</u>	<u>0.1634</u>
lh sag	28	22.25	22.01	8.67	23	22.84	23.30	8.64	42	25.06	28.05	9.91	<u>0.2529</u>	<u>0.3469</u>
rheobase	28	52.16	44.86	30.90	23	70.86	69.81	36.43	41	69.31	69.81	37.54	<u>0.0654</u>	<u>0.9917</u>
ISI (ratio 1/6)	27	2.55	2.32	1.00	22	2.39	2.11	0.68	42	1.98	1.86	0.47	<u>0.0038</u>	<u>0.0123</u>
maxAP	27	12.04	11.00	2.59	22	9.77	10.00	2.05	42	10.52	10.00	2.48	<u>0.0044</u>	0.2278
lhalfmaxAP	27	102.40	96.82	39.97	22	122.20	120.10	32.56	42	122.90	116.30	46.33	<u>0.0576</u>	<u>0.6471</u>
AP thesh	28	-39.00	-38.45	2.75	23	-38.30	-38.70	3.75	42	-36.91	-36.54	3.41	<u>0.0163</u>	<u>0.0457</u>
AP amp.	28	84.98	86.78	10.90	23	88.85	90.03	7.73	42	90.29	91.51	6.92	<u>0.0396</u>	<u>0.4537</u>
AP hw	28	2.05	2.04	0.26	23	1.91	1.88	0.21	42	1.94	1.91	0.21	<u>0.0546</u>	<u>0.5371</u>
AP rise	28	0.54	0.54	0.12	23	0.50	0.49	0.07	42	0.46	0.45	0.08	<u>0.0013</u>	<u>0.0103</u>
AP decay	28	2.19	2.19	0.41	23	2.07	2.03	0.31	42	2.19	2.20	0.27	<u>0.2392</u>	0.1174
EPSP amp.	27	0.59	0.59	0.08	22	0.59	0.59	0.10	42	0.61	0.58	0.12	<u>0.8246</u>	<u>0.5555</u>
EPSP frequ.	27	0.47	0.31	0.61	22	0.49	0.32	0.50	42	0.40	0.25	0.41	<u>0.6986</u>	<u>0.3858</u>

multiple comparisons:	ISI (ratio 1/6)	Ank-G-GFP+Cre is different from both others
significant pairs:	maxAP	wildtype is different from both Ank-G-GFP groups
	AP thesh	wildtype vs. ankG-GFP+Cre
	AP amp.	wildtype is different to ankG-GFP+Cre
	AP rise	wildtype vs ankG-GFP+Cre

Supplementary Table 2 Summary of Cre viruses and Cre driver lines

Neuron population	Cre virus / line	Common name	Source, strain
Unspecific	FUW-nGFP::Cre (lentiviral vector), CMV promotor	nGFP-Cre, NA	Gift from the Südhof lab, Stanford University, CA, USA
Unspecific	FUW-nGFP:: ΔCre (lentiviral vector), CMV promotor	nGFP-ΔCre, NA	Gift from the Südhof lab, Stanford University, CA, USA
Excitatory neurons	pENN.AAV.CamKII 0.4.Cre.SV40	CaMKII-Cre	Addgene viral prep #105558-AAV5, Lot: v7050
Neurons (unspecific)	ENN.AAV.hSyn.Cre.WPRE.hGH	Synapsin-Cre	Addgene viral prep #105553-AAV1, Lot: v75882
Inhibitory neurons	AAV1-hDlx-Flex-dTomato-Fishell_7	hDlx-tdTomato	Addgene viral prep #83894-AAV1
Neurons (unspecific)	pAAV-hSyn-Cre-P2A-dTomato	Synapsin-Cre-tdTomato	Addgene viral prep 107738-AAVrg, Lot: v75881
Excitatory neurons	B6.Cg-Tg(Camk2a-Cre)T29-1Stl/J	T29-1 IMSR_JAX:005359	The Jackson Laboratory Strain # 005359
Parvalbumin-pos. interneurons with tdTomato	B6;129P2-Pvalb ^{tm1(Cre)Arbr/J} crossed with B6.Cg-GT(ROSA)26Sor ^{tm14(CAG-tdTomato)Hze/J}	B6 PV ^{Cre} IMSR_JAX:017320 Ai14 IMSR_JAX:007914	The Jackson Laboratory Strain # 017320 Strain # 007914
Unspecific	AAV-retro/2-hSyn1-mCherry-iCre-WRPE-hGHP(A)	Retro-mCherry-Cre	University of Zürich, Viral Vector Facility, v230

Supplementary Table 3 Specification of primary and secondary antibodies (catalog number, working dilution, previously conducted controls, sources, Research Resource Identification Portal (RRID) code and references where available).

Primary Antibody Clone/type	Dilution	Reported controls				Source & Catalog Number RRID or other reference
		KO	IF	IP	WB	
<i>Ankyrin-G</i> (rb)	1:500		X		X	Santa Cruz Biotechnology, Heidelberg, Germany; sc-28561 AB_633909
<i>Ankyrin-G</i> (gp)	1:1000		X		X	Synaptic Systems, Göttingen, Germany 386 005 [1]
<i>Ankyrin-G</i> (ms) N106/36	1:500	X	X		X	UC Davis/NIH NeuroMab Facility, CA, USA; 73-146 AB_2315803
<i>ank-G C-terminus</i>	1:200		X			Santa Cruz Biotechnology, Heidelberg, Germany; sc-28561; discontinued
<i>βIV-spectrin</i> (rb)	1:1000	X	X		X	Self-made [2-4]
<i>Caspr</i> (ms) K65/35	1:500	X	X	X	X	UC Davis/NIH NeuroMab Facility, CA, USA; 75-001 AB_2083496
<i>FGF14</i> (ms) N56/21	1:500	X	X	X	X	UC Davis/NIH NeuroMab Facility, CA, USA; 75-096 AB_2104060
<i>GFP</i> (ch)	1:1000		X			Acris Antibodies GmbH, Hiddenhausen, Germany; AP20142PU-N AB_10756183
<i>Iba1</i> (rb)	1:2000		X			Wako, Neuss, Germany; 019-19741 AB_839504
<i>Kv1.2</i> (ms) K14/16	1:200	X	X	X	X	UC Davis/NIH NeuroMab Facility, CA, USA; 73-008 AB_2296313
<i>Kv2.1</i> (ms) K89/34	1:1000	X	X		X	UC Davis/NIH NeuroMab Facility, CA, USA; 75-014-020 AB_2877280
<i>Nav1.6</i> (rb)	1:2000		X		X	Alomone Labs, Jerusalem, Israel ASC-009 AB_2040202
<i>NeuN</i> (ms) A60	1:500		X		X	Millipore, Temecula, CA, USA; MAB377 AB_2314889
<i>NeuN</i> (gp)	1:2000		X			Synaptic Systems, Göttingen, Germany 266 004 AB_2619988
<i>Parvalbumin</i> (rb)	1:500		X		X	Swant Inc., Marly, Switzerland PV27 AB_2631173
<i>Synaptopodin</i> (gp)	1:500		X		X	Synaptic Systems, Göttingen, Germany 163 004 AB_10549419
<i>TRIM46</i> (ms) <i>SMP14</i> (aka <i>MDM2</i>)	1:500		X		X	Santa Cruz Biotechnology, Heidelberg, Germany; sc-965 AB_627920
<i>vGAT</i> (ch)	1:1000		X			Synaptic Systems, Göttingen, Germany 131 006 AB_2619820

KO absence of immunosignal in knock out animals, IF immunofluorescence, IP immuno-precipitation, WB western blot, rb rabbit, ms mouse, gp guinea pig, ch chicken

Supplementary Table 3 (continued) Specification of primary and secondary antibodies (catalog number, working dilution, previously conducted controls, sources, Research Resource Identification Portal (RRID) code and references where available).

Secondary Antibody Clone/type	Dilution	Reported controls				Source & Catalog Number RRID or other reference
		KO	IF	IP	WB	
<i>FluoTag-X4-anti GFP-StarRED</i> 1H1/1B2	1:500					NanoTag Technologies, Göttingen, Germany; N0304 AB_2744631
<i>gt anti mouse abberior STAR 580</i>	1:100					Abberior GmbH, Göttingen, Germany; ST580-1001 AB_2923543
<i>gt anti rabbit abberior STAR 580</i>	1:100					Abberior GmbH, Göttingen, Germany; ST580-1002 AB_2910107
<i>gt anti ch Alexa Fluor 488</i>	1:1000					Molecular Probes, Thermo Fisher, Karlsruhe, Germany; A-11039 AB_42924
<i>gt anti ms Alexa Fluor 568</i>	1:1000					Molecular Probes, Thermo Fisher, Karlsruhe, Germany; A-11004 AB_143162
<i>gt anti rb Alexa Fluor 568</i>	1:1000					Molecular Probes, Thermo Fisher, Karlsruhe, Germany; A-21069 AB_141416
<i>gt anti gp Alexa Fluor 568</i>	1:1000					Molecular Probes, Thermo Fisher, Karlsruhe, Germany; A-11075 AB_141954
<i>gt anti ch Alexa Fluor 568</i>	1:1000					Molecular Probes, Thermo Fisher, Karlsruhe, Germany; A-11041 AB_2534098
<i>gt anti ms Alexa Fluor 594</i>	1:500					Molecular Probes, Thermo Fisher, Karlsruhe, Germany; A-21125 AB_141593
<i>gt anti rb Alexa Fluor 594</i>	1:500					Molecular Probes, Thermo Fisher, Karlsruhe, Germany; A-11012 AB_141359
<i>gt anti ms Alexa Fluor 647</i>	1:500					Molecular Probes, Thermo Fisher, Karlsruhe, Germany; A AB_2535804-21235
<i>gt anti rb Alexa Fluor 647</i>	1:500					Molecular Probes, Thermo Fisher, Karlsruhe, Germany; A-21244 AB_2535812
<i>gt anti gp Alexa Fluor 647</i>	1:500					Molecular Probes, Thermo Fisher, Karlsruhe, Germany; A-21450 AB_2735091
<i>gt anti ch Alexa Fluor 647</i>	1:500					Molecular Probes, Thermo Fisher, Karlsruhe, Germany; A-21449 AB_2535866
<i>Alexa Streptavidin 568</i>	1:1000					Molecular Probes, Thermo Fisher, Karlsruhe, Germany; S11226 AB_2315774

KO absence of immunosignal in knock out animals, IF immunofluorescence, IP immuno-precipitation, WB western blot, rb rabbit, ms mouse, gp guinea pig, ch chicken

Supplementary Table 4 Summary of fixation and blocking reagents for all immunofluorescence experiments.

Sample	Fixation Time / DIV	Post Fix	Blocking buffer Incubation buffer
Isolated hippocampal neurons	4% PFA, 15 min DIV 19	No	B: 1% BSA in PBS. Prior to blocking, quench in PBS with 100 mM glycine, 100 mM ammonium chloride (5 min) and application of 0.1% Triton X-100 for 5 min I: PBS
Hippocampal OTC	4% PFA, 30 min	No	B: 0.1% Triton X-100, 1% BSA, 0.2% fish skin gelatine, in 1 x PBS I: same
<i>Ex vivo</i> acute slices	2% PFA, 90 min	No	B: 0.3% Triton X-100, 5% normal goat serum in 1 x PBS I: 0.2% Triton X-100, 1% normal goat serum in 1 x PBS
Whole mount retina	4% PFA, 15 min >P55	No	B: 0.5% Triton X-100, 0.2% BSA, 0.02% sodium azide in 1x PBS I: 1% Triton X-100, 10% FCS and 0.02% sodium azide in 1x PBS
Cryosections	Perfusion, 15 min 2% PFA (for ion channels) 4% PFA (for all others) >P28	No	B: 1% BSA, 0.2% fish skin gelatine, 0.1% Triton X-100 in 1 x PBS I: same

PFA paraformaldehyde, *min* minutes, *DIV* days in vitro, *BSA* bovine serum albumin, *PBS* phosphate buffered saline, *FCS* fetal calf serum

References for Supplements

- Schlüter, A., et al., Dynamic regulation of synaptopodin and the axon initial segment in retinal ganglion cells during postnatal development *Frontiers Cell Neurosci*, 2019.
- Gutzmann, A., et al., A period of structural plasticity at the axon initial segment in developing visual cortex. *Front Neuroanat*, 2014. 8: p. 11.
- Freal, A., et al., Cooperative Interactions between 480 kDa Ankyrin-G and EB Proteins Assemble the Axon Initial Segment. *J Neurosci*, 2016. 36(16): p. 4421-33.
- Höflin, F., et al., Heterogeneity of the Axon Initial Segment in Interneurons and Pyramidal Cells of Rodent Visual Cortex. *Front Cell Neurosci*, 2017. 11: p. 332.